Radiative transfer codes for atmospheric correction and aerosol retrieval: intercomparison study

Svetlana Y. Kotchenova,[1,*] Eric F. Vermote,[1] Robert Levy,[2,3] and Alexei Lyapustin[4]

[1]Department of Geography, University of Maryland, 4321 Hartwick Road, Suite 209, College Park, Maryland 20740, USA

[2]Science Systems and Applications, Inc., 10210 Greenbelt Road, Suite 600, Lanham, Maryland 20706

[3]NASA Goddard Space Flight Center, Climate and Radiation Branch, Code 613.2, Greenbelt, Maryland 20771, USA

[4]University of Maryland Baltimore County, Goddard Earth Science Technology Center and NASA Goddard Space Flight Center, Code 614.4, Greenbelt, Maryland 20771, USA

*Corresponding author: skotchen@ltdri.org

Received 3 January 2008; revised 15 March 2008; accepted 17 March 2008; posted 17 March 2008 (Doc. ID 91149); published 24 April 2008

Results are summarized for a scientific project devoted to the comparison of four atmospheric radiative transfer codes incorporated into different satellite data processing algorithms, namely, 6SV1.1 (second simulation of a satellite signal in the solar spectrum, vector, version 1.1), RT3 (radiative transfer), MODTRAN (moderate resolution atmospheric transmittance and radiance code), and SHARM (spherical harmonics). The performance of the codes is tested against well-known benchmarks, such as Coulson's tabulated values and a Monte Carlo code. The influence of revealed differences on aerosol optical thickness and surface reflectance retrieval is estimated theoretically by using a simple mathematical approach. All information about the project can be found at http://rtcodes.ltdri.org.

OCIS codes: 290.1310, 010.1300.

1. Introduction

Radiative transfer (RT) codes simulating the propagation of radiation through the atmosphere serve as cornerstones for satellite remote sensing. They are used in a number of different applications (e.g., atmospheric correction [1,2], atmosphere–ocean interactions [3], and parameterization for the directional reflectance of broken cloud fields [4]) and are gradually replacing semiempirical and empirical approaches by providing more accurate and mathematically justified solutions.

The importance of RT codes for remote sensing science constitutes the major reason for their extensive validation. Upon its development, a RT code usually undergoes some preliminary testing to determine the quality of its performance. In addition, special code comparison studies are carried out to estimate performance and characteristics of different RT codes [5–9]. The most comparable characteristics include accuracy and speed. User friendliness is desirable but not strictly required. Such studies have proved to be useful, as they facilitate the user's choice between codes. However, they have to be performed on a regular basis in view of the fact that a particular RT code may undergo significant improvements during relatively short periods of time.

These studies are also important for the field of passive remote sensing, where RT codes are used mostly for calculation of lookup tables (LUTs) or precomputed sets of values (e.g., reflectance) for satellite data processing algorithms. Created LUTs are then applied to solve both direct and inverse problems. The former implies calculation of radiance (reflectance) at the top (or bottom) of the atmosphere on the basis of known atmospheric parameters, while the latter involves retrieval of atmospheric properties based on given radiance (reflectance) values.

One can say that the accuracy of LUTs directly depends on the code used for their creation. In the field

0003-6935/08/132215-12$15.00/0

of pure simulation studies the general atmospheric RT code accuracy requirement is 1%.[10] This boundary, however, is often lowered depending on the type of application. Thus, it would be interesting to find out whether violation of this requirement had a significant effect on the resulting satellite product.

To address the above-stated issues, we have executed a joint project devoted to the comparison and evaluation of four atmospheric RT codes incorporated into different satellite data processing algorithms, namely, (1) 6SV1.1 (second simulation of a satellite signal in the solar spectrum, vector, version 1.1) [11], which is a basic code of the MODIS (moderate resolution imaging spectroradiometer) atmospheric correction algorithm [1]; (2) RT3 (radiative transfer) [12], a polarized code underlying the MODIS coarse-resolution (10 km) aerosol retrieval algorithm [13]; (3) MODTRAN (moderate resolution atmospheric transmittance and radiance code) [14,15], a scalar code used for the analysis of AVIRIS (airborne visible/infrared imaging spectrometer) data [16]; and (4) SHARM (spherical harmonics) [17], another scalar code that underlies the MAIAC (multiangle implementation of atmospheric correction for MODIS) algorithm [2].

The main goals of the project are (1) to evaluate the accuracy of each code in comparison with standard benchmark references such as Coulson's tabulated values [18] and a Monte Carlo approach [4], (2) to illustrate differences between individual simulations of the codes, (3) to determine how the revealed differences influence the accuracy of aerosol optical thickness (AOT) and surface reflectance retrievals, and (4) to create reference (benchmark) data sets that can be used in future code comparison studies. All information about this project, including the descriptions of the codes, conditions, and results (presented in the form of Excel files and graphs) of the comparison, and references to relevant publications, is posted on the official project Web site [19].

This paper may be considered a scientific report that summarizes the results of the project in addition to the provided site. Section 2 contains short technical descriptions of the codes and benchmarks used. Sections (3)–(5) describe the conditions and main results of the comparison for molecular, aerosol, and realistic (molecular + aerosol) atmospheres, respectively. In each case, top-of-the-atmosphere (TOA) reflectance values are produced as outputs of the codes. Section 6 discusses what effect errors in RT simulations have on the AOT and surface reflectance retrievals, and Section 7 provides concluding remarks.

2. Description of Codes and Benchmarks

6SV1 is an advanced RT code developed by the MODIS LSR SCF (Land Surface Reflectance Science Computing Facility). It simulates the reflection of solar radiation by a coupled atmosphere–surface system for a wide range of atmospheric, spectral, and geometric conditions. The code operates on the basis of a successive orders of scattering method and accounts for the polarization of radiation in the atmosphere through the calculation of the Q and U components of the Stokes vector. It is publicly available at http://6s.ltdri.org. This site also contains two manuscripts summarizing the code validation effort [20,21], information on recent updates, the code manual [22], and a link to a special Web interface that can help an inexperienced user build necessary input files.

MODTRAN is a scalar RT code developed by the Air Force Research Laboratory in collaboration with Spectral Sciences, Incorporated [14]. The code calculates atmospheric transmittance and radiance and efficiently simulates molecular and cloud-aerosol emission. It assumes a stratified atmosphere and a spherical earth surface (which can be transformed into plane parallel by setting the Earth radius to an extremely large value). Different atmospheric characteristics, such as temperature, pressure, and atmospheric species concentrations, need to be specified at the boundaries of each layer. The DISORT (discrete ordinates) code [23,24] is used as a subroutine in MODTRAN to enable the azimuth dependence of multiple scattering. The latest publicly released version of the code is MOD4v3r1 (MODTRAN 4 version 3 revision 1), which is available by request at http://www.kirtland.af.mil/library/factsheets/factsheet.asp?id=7915.

RT3 is a fully polarized atmospheric RT model created by Evans and Stephens [12]. It operates in both vector and scalar modes by calculating monochromatic radiation emerging from the top of a plane-parallel, vertically inhomogeneous scattering atmosphere consisting of randomly oriented particles. The user can choose between solar and thermal sources of radiation. The code is written on the basis of the doubling–adding approach, which is considered numerically stable for large optical depths. It is publicly available at http://nit.colorado.edu/polrad.html. Here we will use RT3 only in vector mode.

SHARM is a plane-parallel scalar RT code originally formulated by Muldashev *et al.* [10] and significantly improved later by Lyapustin [17]. The code performs simultaneous computations of monochromatic radiance and fluxes in the shortwave spectral region for arbitrary view geometries and multiple wavelengths. It is based on the method of spherical harmonics and currently does not take polarization into account. In this comparison study, we use the SHARM–Mie version of the code, which was developed for calculations with spherical aerosol particles. The code can be downloaded from ftp://ltpftp.gsfc.nasa.gov/projects/asrvn/.

Coulson's tabulated values represent accurate calculations of solar radiation reflected and transmitted by a plane-parallel, nonabsorbing molecular atmosphere according to Rayleigh's law [18]. They are used mainly as a benchmark reference to verify the accuracy of a vector RT code [12,25]. The sets of tables selected for this study include relative radiance values emerging from the TOA, calculated with five-digit accuracy.

The Monte Carlo code used in this study is a three-dimensional ray-tracing code written on the basis of the Stokes vector approach. Within this code, the atmospheric path of each individual photon is simulated with the help of probabilistic methods, and components of the Stokes vector are changed accordingly after each interaction of a photon with a molecule or an aerosol particle. The code was primarily developed by Bréon [4] for modeling atmosphere–ocean interactions and was modified later by the MODIS LSR SCF to be used in the 6SV1 validation studies. The modified version can be obtained from the MODIS LSF SCF by request. A Monte Carlo approach often serves as a benchmark for testing other RT methods [26,27].

3. Molecular Atmosphere

A. Conditions of Comparison

The comparison scheme for the case of a molecular atmosphere is shown in Fig. 1. All the codes were tested against Coulson's tabulated values [18], and 6SV1 was separately tested against the Monte Carlo code [4]. The Monte Carlo code served as an auxiliary benchmark in this part of the study, as comparison with Coulson's tables is sufficient to make conclusions about the accuracy of a tested code. In addition, the comparison of 6SV1 and Monte Carlo codes for a molecular atmosphere bounded by Lambertian and anisotropic surfaces was already covered in the 6SV1 validation studies [20,21].

The conditions for the comparison with Coulson's tabulated values are listed in Table 1. Their selection was limited to the conditions provided in Coulson's tables. In total, we selected three values of molecular optical thickness $\tau_{\mathrm{mol}} = \{0.1; 0.25; 0.5\}$, which approximately correspond to the wavelengths $\lambda = \{530; 440; 360\}$ nm, respectively, two values of Lambertian surface reflectance $\rho_{\mathrm{surf}} = \{0.0; 0.25\}$, six values of SZA (solar zenith angle), three values of AZ (relative azimuth), and all available VZAs (view zenith angles).

Comparison with the Monte Carlo code was performed for $\tau_{\mathrm{mol}} = 0.25$, $\rho_{\mathrm{surf}} = \{0.0; 0.25\}$, and SZA $= \{0.0°; 23.0°; 50.0°\}$. 6SV1 TOA reflectances were integrated over the Monte Carlo solid angles. The applied integration procedure is described in detail in the first 6SV1 validation study [20].

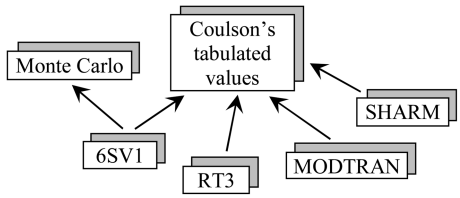

Fig. 1. Comparison scheme for a molecular atmosphere.

It should be noted that the straightforward Monte Carlo approach used in this study is generally considered impractical for the solution of more complicated problems, e.g., the modeling of radiance reflected by clouds, which are characterized by strongly forward-peaked scattering phase functions and a high percentage of multiple scattering [8]. There are more advanced Monte Carlo techniques, such as maximum cross section or local estimate, that do not require sampling of photons in a cone and significantly reduce variance and speed up computational runs. However, Monte Carlo codes utilizing these techniques do not currently take polarization into account.

While 6SV1, MODTRAN, and SHARM can accept any Sun-view geometry configuration, RT3 offers the user an option to select a VZA geometry from several built-in distributions. For this reason, RT3 TOA reflectance values obtained for 56 Gaussian angles were linearly interpolated over the Coulson VZA values. Also, since RT3 includes no anisotropic surface model, the comparison was performed for black and Lambertian surfaces. The selected values of τ_{mol} were manually fixed in the codes to avoid inconsistencies due to slightly different methods for τ_{mol} calculation.

B. Results of Comparison

1. *All Codes versus Coulson's Values*

The results of the comparison with Coulson's tabulated values are illustratively summarized in Fig. 2. Here we calculated the average of the absolute values of relative differences between each RT code and Coulson's values as a function of VZA for each particular case of τ_{mol} and ρ_{surf}. For example, if we consider a molecular atmosphere with $\tau_{\mathrm{mol}} = 0.1$ bounded by a black surface (column 2 in Table 1), then the y value corresponding to a particular x value (or VZA value) in Fig. 2(a) is the average of the absolute values of relative differences calculated for nine combinations of SZA and

Table 1. Conditions of Comparison with Coulson's Tabulated Values for a Molecular Atmosphere[a]

Condition	$\tau_{\mathrm{mol}}(\lambda, \mathrm{nm})$					
	0.1 (530)		0.25 (440)		0.5 (360)	
ρ_{surf}	0.0	0.25	0.0	0.25	0.0	0.25
SZA, deg	23.0739	0.0	0.0	23.0739	23.0739	0.0
	53.1301	36.8699	36.8699	53.1301	53.1301	36.8699
	78.4630	66.4218	66.4218	78.4630	78.4630	66.4218

[a]Here τ_{mol} is the molecular optical thickness, λ is the wavelength, ρ_{surf} is the surface reflectance, and SZA is the solar zenith angle. VZA (view zenith angle) values (degrees) are from Coulson's tables, and AZ (relative azimuth) is 0.0°, 90.0°, or 180°.

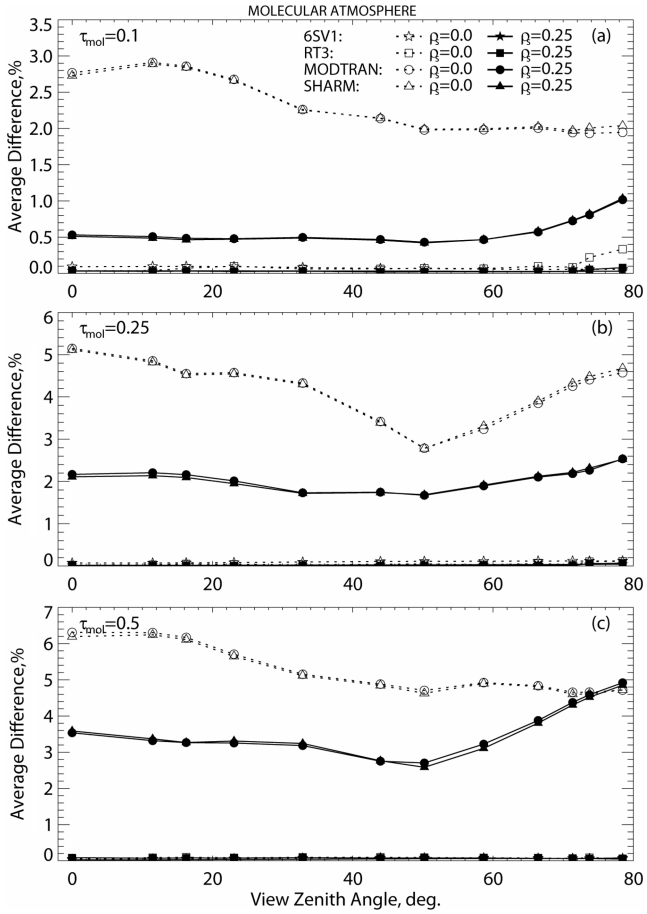

Fig. 2. Results of the comparison with Coulson's tabulated values for a molecular atmosphere with the optical thickness $\tau_{\text{mol}} = \{0.1; 0.25; 0.5\}$ bounded by a Lambertian surface with the reflectance $\rho = \{0.0; 0.25\}$. The geometrical configurations used are listed in Table 1. Note that the errors of 6SV1 and RT3 are too small to be distinctively seen in the plots.

AZ. Also, the difference is called "relative" because it was calculated as a percentage, using Coulson's values as a reference.

Summarizing the above explanation, a mathematical formula for calculating the average of the absolute values of relative differences, $\delta_{\text{mol}}(\theta_v, \tau_{\text{mol}}, \rho_{\text{surf}})$, can be written as follows:

$$\delta_{\text{mol}}(\theta_v, \tau_{\text{mol}}, \rho_{\text{surf}}) = \frac{1}{9}\sum_{\text{SZA}}\sum_{\text{AZ}} \times \frac{|\rho^{\text{Coul}}(\theta_s, \theta_v, \phi, \tau_{\text{mol}}, \rho_{\text{surf}}) - \rho^{\text{code}}(\theta_s, \theta_v, \phi, \tau_{\text{mol}}, \rho_{\text{surf}})|}{\rho^{\text{Coul}}(\theta_s, \theta_v, \phi, \tau_{\text{mol}}, \rho_{\text{surf}})} \times 100\%, \quad (1)$$

where θ_s is the SZA, θ_v is the VZA, ϕ is the relative AZ, $\rho^{\text{Coul}}(\theta_s, \theta_v, \phi, \tau_{\text{mol}}, \rho_{\text{surf}})$ is the TOA reflectance derived from Coulson's tables for a given set of input parameters, and $\rho^{\text{code}}(\theta_s, \theta_v, \phi, \tau_{\text{mol}}, \rho_{\text{surf}})$ is the TOA reflectance calculated by a given RT code.

6SV1 and RT3 show excellent agreement with Coulson's values. The 6SV1 average difference stays within 0.13% for all three values of τ_{mol}, in accordance with the results of its validation studies [20,21]. The RT3 average difference does not exceed 0.34% for $\tau_{\text{mol}} = 0.1$ and stays within 0.12% for $\tau_{\text{mol}} = \{0.25; 0.5\}$. Note that these errors are too small to be seen distinctively in Fig. 2.

SHARM and MODTRAN do not agree well with Coulson's tabulated values, as neither of them take polarization into account. This confirms the results of previous studies that stated that neglecting the effects of polarization would induce large errors in simulations for Rayleigh atmosphere [28,29]. However, these codes agree very well (within 0.3%) with each other.

2. *6SV1 versus Monte Carlo*

The results of the comparison between 6SV1 and Monte Carlo codes are presented in Fig. 3. Differences between the codes fluctuate around the zero line in an arbitrary way with maximum absolute deviations of 0.45% for $\rho_{\text{surf}} = 0.0$ and 0.3% for $\rho_{\text{surf}} = 0.25$. Here we applied a more accurate integration of 6SV1 outputs over larger Monte Carlo solid angles, which led to a better agreement between the codes, compared with the findings in the 6SV1 validation studies.

S4. Aerosol Atmosphere

A. Conditions of Comparison

The comparison scheme for an aerosol atmosphere is shown in Fig. 4. First, 6SV1 was tested against Monte Carlo, and then RT3, MODTRAN, and SHARM were tested against 6SV1. The rationale behind this scheme is explained in Subsection 4.B.

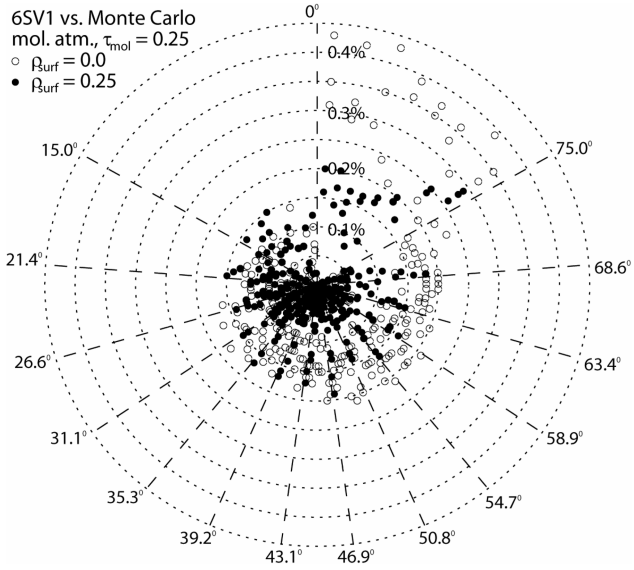

Fig. 3. Results of the comparison between 6SV1 and Monte Carlo for a molecular atmosphere with $\tau_{\text{mol}} = 0.25$ bounded by a Lambertian surface with $\rho_{\text{surf}} = \{0.0; 0.25\}$. SZA $= \{0.0; 23.0°; 50.0°\}$. The hemispherical space at the TOA is divided into a number of solid angles. The boundary VZA angles are shown as angular coordinates. The AZ space is equally divided into eight angles. The radius coordinate designates the relative difference between 6SV1 and Monte Carlo TOA reflectances.

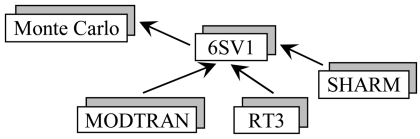

Fig. 4. Comparison scheme for aerosol and mixed atmospheres.

Three aerosol types described in the Dubovik *et al.* study [30], namely, an urban–industrial aerosol and two biomass burning smoke aerosols with different degrees of absorption, were selected for this study. Their characteristics are provided in Table 2. The biomass burning smoke parameters were retrieved from AERONET (Aerosol Robotic Network) measurements collected over African savanna and Amazonian tropical forest regions. The former is characterized by the highest observed aerosol absorption, while the latter can be noted for the lowest one. The urban–industrial parameters were extracted from AERONET measurements taken over the GSFC (Goddard Space Flight Center) site in Maryland. Hereinafter, the selected aerosol models will simply be referred to as AS (African savanna), AF (Amazonian forest), and UI (urban–industrial).

In total, three wavelengths were selected for the study: $\lambda = \{412; 670\}$ nm. The first one is a basic wavelength for retrieval of aerosol properties over bright targets, such as arid, semiarid and urban areas [31]. The other two are among four AERONET wavelengths. They approximately match the MODIS spectral bands 1 and 3 (centered at 470 and 648 nm), used for retrieval of aerosol properties over ocean surfaces and dark vegetation targets.

The AOT τ_{aer} was manually fixed in all codes to $\{0.2; 0.8\}$ for the AS and UI models and to $\{0.2; 0.8; 2.0\}$ for the AF model, in accordance with the measured ranges of variation. The required aerosol scattering phase functions were calculated on the basis of the provided particle distributions. While both 6SV1 and SHARM have built-in algorithms to perform their own Mie calculations, other codes lack such algorithms and require that phase function values be provided as input. For example, RT3 might be combined with the Mie vector code (MIEV) developed by Wiscombe [32].

However, since the available Mie algorithms showed a slight disagreement between calculated values, it was decided to manually input phase function values calculated by 6SV1 into RT3 and SHARM. Thus, two types of calculation were finally performed for these two codes: those with their own Mie algorithms and those with the 6SV1 Mie computations. MODTRAN was filled with scalar aerosol phase functions calculated by SHARM, and Monte Carlo was complemented with vector phase functions calculated by 6SV1.

The geometric conditions for the comparison of RT3, MODTRAN, and SHARM with 6SV1 are provided in Table 3. As in the case of a molecular atmosphere, RT3 outputs need to be interpolated over the selected VZA values. The comparison between 6SV1 and Monte Carlo was performed for SZA $= \{0.0°; 23.0°; 50.0°\}$. The 6SV1 outputs were integrated over the Monte Carlo solid angles. For the sake of time, we did not compare 6SV1 with Monte Carlo for all study cases. Instead, we used only one wavelength for each model: 412 nm for AS, 440 nm for UI, and 670 nm for AF, and two values of $\tau_{\text{aer}} = \{0.2; 0.8\}$.

This part of the study did not involve background other than a black surface. Incorporation of a Lambertian surface was well tested in the case of a molecular atmosphere. The comparison for a pure aerosol atmosphere usually needs to be completed to estimate the significance of errors caused by asymmetric scattering before one can proceed to processing realistic cases of a mixed atmosphere.

B. Results of the Comparison

1. *6SV1 versus Monte Carlo*

Here we show the results of the comparison between 6SV1 and Monte Carlo for the UI aerosol model, $\lambda =$ 412 nm and $\tau_{\text{aer}} = \{0.2; 0.8\}$ (Fig. 5). All other results are provided on the project Web site [19] in the form of Excel files. 6SV1 demonstrates good agreement

Table 2. Parameters of Aerosol Models Used in the Comparison[a]

Parameter	Model		
	Urban–Industrial and Mixed	Biomass Burning	Biomass Burning
Location	GSFC, Greenbelt, Md. (1993–2000)	Amazonian forest, Brazil (1993–1994), Bolivia (1998–1999)	African savanna, Zambia (1995–2000)
Range of τ_{aer}	$0.1 \le \tau(440) \le 1.0$	$0.1 \le \tau(440) \le 3.0$	$0.1 \le \tau(440) \le 1.5$
Values of τ_{aer} selected for this study	0.2; 0.8	0.2; 0.8; 2.0	0.2; 0.8
Refractive index: real part; imaginary part	$1.41 - 0.03\tau(440); 0.003$	1.47; 0.0093	1.51; 0.021
SSA at $\lambda = 412, 440, 670$ nm	0.97, 0.98, 0.97	0.94, 0.94, 0.93	0.88, 0.88, 0.84
r_{Vf}, μm	$0.12 + 0.11\tau(440)$	$0.14 + 0.013\tau(440)$	$0.12 + 0.025\tau(440)$
σ_f, μm	0.38	0.40	0.40
r_{Vc}, μm	$3.03 + 0.49\tau(440)$	$3.27 + 0.58\tau(440)$	$3.22 + 0.71\tau(440)$
σ_c, μm	0.75	0.79	0.73
$C_{\text{Vf}}, \mu\text{m}^3/\mu\text{m}^2$	$0.15\tau(440)$	$0.12\tau(440)$	$0.12\tau(440)$
$C_{\text{Vc}}, \mu\text{m}^3/\mu\text{m}^2$	$0.01 + 0.04\tau(440)$	$0.05\tau(440)$	$0.09\tau(440)$

[a]All parameters except SSA (single scattering albedo) at $\lambda = 412$ nm were extracted from the Dubovik *et al.* study [30]. SSA at 412 nm was calculated by 6SV1. Here τ_{aer} is the AOT, λ is the wavelength, r_{Vf} and r_{Vc} are mean volumetric radii, σ_f and σ_c are standard deviations, and C_{Vf} and C_{Vc} are particle volume concentrations of fine and course modes.

Table 3. Geometric Conditions for the Comparison of RT3, MODTRAN, and SHARM with 6SV1 for an Aerosol Atmosphere[a]

VZA, deg				
$\tau_{aer} = 0.2$	$\tau_{aer} = 0.8$	$\tau_{aer} = 2.0$	SZA, deg	AZ, deg
As in Coulson's tables	From 5.0° to 80.0° with a step of 5°	From 3.0° to 70.0° with a step of 5°	0.0° 10.0° 23.0709° 45.0° 58.6677° 75.0°	0.0° 90.0° 180.0°

[a]The symbols and abbreviations used are explained in the captions for Tables 1 and 2.

with Monte Carlo. In all studied cases, the absolute values of its maximum relative error do not exceed 1%. As in the case of a molecular atmosphere, a more accurate integration of 6SV1 values significantly improved agreement between the codes for the last two solid angles.

Since 6SV1 is capable of providing simulations that are as accurate as those performed by the benchmark Monte Carlo, 6SV1 can be used as the benchmark itself. The Monte Carlo code is not well suited for testing studies. Besides being extremely time consuming, it also requires that outputs of a tested code be produced at a high angular resolution (e.g., 100 6SV1 values need to be calculated for one Monte Carlo solid angle) to achieve accurate integration over its solid angles. Thus, it would be more convenient to replace Monte Carlo with another RT code that is as accurate as Monte Carlo and can handle a specific Sun-view geometry configuration.

2. *RT3, MODTRAN, and SHARM versus 6SV1*

The results of the comparison of RT3, MODTRAN, and SHARM with 6SV1 are shown in Fig. 6 for the UI aerosol model and all studied combinations of λ and τ_{aer}.

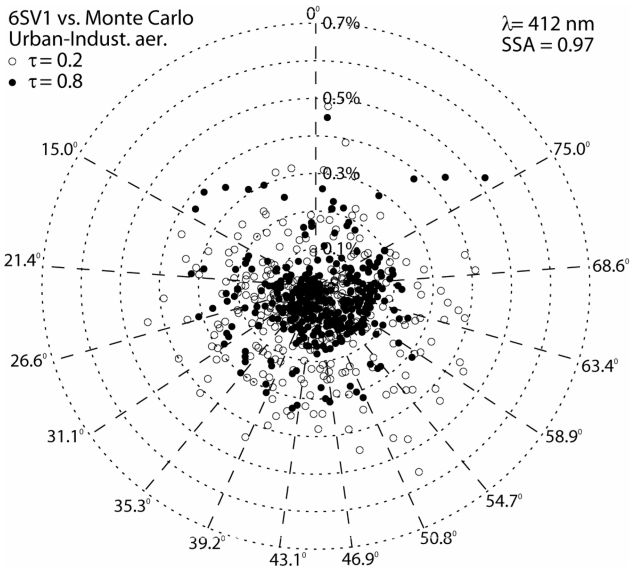

Fig. 5. Results of the testing of 6SV1 against the MC code for the UI aerosol atmosphere with $\tau_{aer} = \{0.2; 0.8\}$, bounded by black surface. SZA $= \{0.0; 23.0°; 50.0°\}$, $\lambda = 412$ nm. The geometric configuration is explained in the caption for Fig. 4.

As in the case of a molecular atmosphere, we calculated the average of the absolute values of relative differences between the outputs of the codes, $\delta_{aer}(\theta_v, \tau_{aer}, \alpha, m_{aer})$, using 6SV1 as the reference. Here α designates single-scattering albedo (SSA), and m_{aer} designates the selected aerosol model. The total number of SZA and AZ angles in this case is equal to 15, as SZA $= 75.0°$ was not included in the calculations for Fig. 6. Also, the 6SV1 scattering phase functions were manually input to SHARM and RT3, which was done as a simple formality, as the difference between the phase functions account on average for disagreement of no more than 0.3%.

Both SHARM and RT3 demonstrate good agreement with 6SV1 at $\lambda = 412$ nm and 440 nm, where the aerosol influence is generally small. The scalar and vector solutions agree within 0.3% at $\tau_{aer} = 0.8$, which confirms that aerosol tends to depolarize radiation. For both codes, the agreement worsens at 670 nm, where the influence of aerosol increases. The difference between SHARM and 6SV1 is clearly caused by the effects of polarization, while the difference observed between RT3 and 6SV1 is attributed to the applied angle interpolation and an insufficient number of calculation angles (28 Gaussian angles were used in the aerosol cases).

MODTRAN does not agree well with 6SV1. The average error stays within approximately 3% at smaller VZA angles and begins to increase sharply with the increase of VZA value. We think that such disagreement arises from the use of only 16 calculation angles (or streams) and the Henyey–Greenstein phase function in the DISORT subroutine of MODTRAN. While the aerosol scattering phase function provided by the user is utilized by MODTRAN for exact single-scattering calculations, it is replaced by the Henyey–Greenstein function for multiple-scattering computations [33], which is modeled by DISORT on the basis of a given asymmetry parameter. It should be noted, however, that DISORT itself can handle an arbitrary number of streams and arbitrary phase functions if it is provided with appropriate Legendre coefficients.

To sustain this assertion, we compared single- and multiple-scattering calculations performed by SHARM and MODTRAN for the UI aerosol, $\lambda =$ 440 nm and $\tau_{aer} = \{0.2; 0.8\}$ (Fig. 7). On average, the codes agree very well (within 0.2% for $\tau_{aer} =$

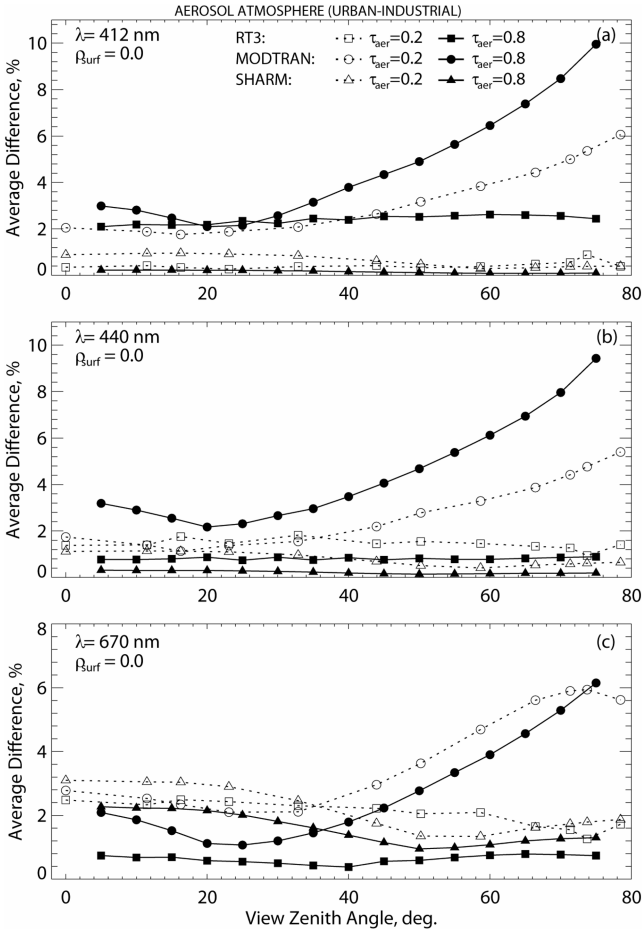

Fig. 6. Results of the comparison of RT3, MODTRAN, and SHARM with 6SV1 for the UI aerosol model for all combinations of λ and τ_{aer} listed in Table 2. 6SV1 is used as a reference code.

0.2 and 0.3% for $\tau_{\mathrm{aer}} = 0.8$) for the whole set of angles in the case of single scattering.

5. Mixed Atmosphere

A. Conditions of Comparison

The comparison scheme for a realistic mixed (aerosol + molecular) atmosphere was similar to that used for an aerosol atmosphere. The conditions of the comparison were also the same except for the fact that a molecular constituent was added to each aerosol model and a Lambertian surface with $\rho = 0.05$ was included in addition to a black surface. The molecular optical thickness was adopted as calculated in 6SV1: $\tau_{\mathrm{mol}} = \{0.303; 0.232; 0.042\}$ for $\lambda = \{412; 440; 670\}$nm, respectively.

For all codes except for MODTRAN we used exponential optical thickness profiles for aerosol and molecular constituents:

$$\tau_{\mathrm{mol}}(z) = \tau_{\mathrm{mol}}(0)\exp(-z/H_{\mathrm{mol}}),$$
$$\tau_{\mathrm{aer}}(z) = \tau_{\mathrm{aer}}(0)\exp(-z/H_{\mathrm{aer}}), \qquad (2)$$

where z is the altitude of an atmospheric calculation layer, and $H_{\mathrm{mol}} = 8\,\mathrm{km}$ and $H_{\mathrm{aer}} = 2\,\mathrm{km}$ are scale

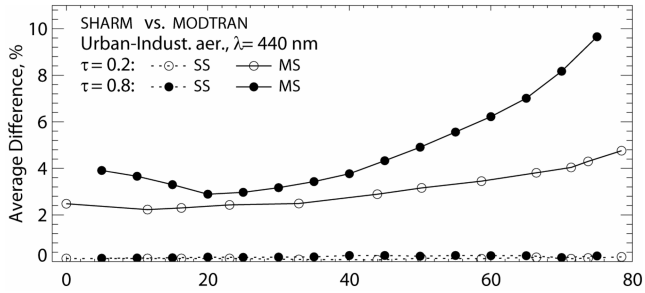

Fig. 7. Results of the comparison between SHARM and MODTRAN for the UI aerosol model for $\lambda = 440$ nm. SS, single scattering; MS, multiple scattering. SHARM is used as a reference code.

heights of molecular and aerosol components. These profiles are used by default in 6SV1. A 1976 U.S. standard model of atmosphere was used in SHARM, which has an equivalent scale height of 8.02 km, but this difference does not affect the results. In each layer, the proportions of molecules (η_{mol}) and aerosol particles (η_{aer}) in the total mixture were defined as

$$\eta_{\mathrm{mol}}(z) = \tau_{\mathrm{mol}}(z)/[\tau_{\mathrm{mol}}(z) + \tau_{\mathrm{aer}}(z)],$$
$$\eta_{\mathrm{aer}}(z) = \tau_{\mathrm{aer}}(z)[\tau_{\mathrm{mol}}(z) + \tau_{\mathrm{aer}}(z)]. \qquad (3)$$

Unfortunately, MODTRAN does not offer an option to input an exponential aerosol profile. The code does offer a possibility to specify as many as four different aerosol models characterized by different values of extinction, absorption and asymmetry parameters, and phase functions, but there is no convenient option to vary τ_{aer} as a function of height. Thus, it was decided to use the code as it is: with a molecular profile defined by the 1976 U.S. standard model, which is almost similar to the default profile used in 6SV1, and with a uniform aerosol layer.

B. Results of the Comparison

1. *6SV1 versus Monte Carlo*

The results are partially illustrated in Fig. 8 by the example of a mixed atmosphere with the AS aerosol constituent, bounded by a black surface. 6SV1 shows very good agreement with Monte Carlo code for both values of AOT. The absolute value of the relative difference stays within 0.7% for $\tau_{\mathrm{aer}} = 0.2$ and within 0.5% for $\tau_{\mathrm{aer}} = 0.8$ for all VZA ranges except the last one, where it goes up to 0.86% for the backscattering direction.

2. *RT3, MODTRAN, and SHARM versus 6SV1*

In accordance with Subsection 5.B.1, Fig. 9 shows the results for the case of a mixed atmosphere with the AS aerosol constituent, bounded by a black surface. SHARM and MODTRAN follow approximately the same behavior pattern. Their agreement with 6SV1 is best at $\lambda = 670\,\mathrm{nm}$ and worsens at shorter wavelengths. The errors of SHARM are those arising from ignoring the effects of polarization. Thus, the

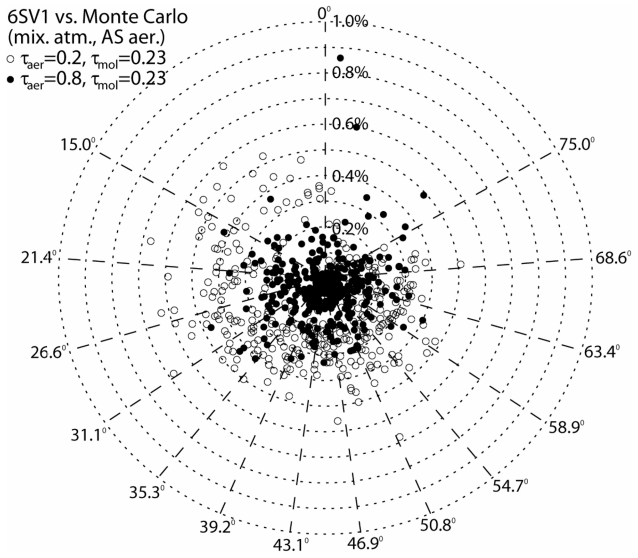

Fig. 8. Results of the testing of 6SV1 against the MC code for a mixed atmosphere bounded by a black surface. The aerosol is presented by the AS model, $\tau_{aer} = \{0.2; 0.8\}$, SZA $= \{0.0; 23.0°; 50.0°\}$, and $\lambda = 412$ nm. The geometric configuration is explained in the caption for Fig. 4.

results of the comparison between SHARM and 6SV1 can be also used to demonstrate the importance of polarization by the atmosphere in RT modeling. In the case of MODTRAN, there are three sources of disagreement: the use of the Henyey–Greenstein function for aerosol modeling, the neglect of the effects of polarization, and the impossibility of inputting the same aerosol profile as in 6SV1.

RT3 demonstrates better agreement with 6SV1. Its average difference with 6SV1 varies within 0.5%–3.0% for all considered cases. We assume that a slightly worse agreement compared with the case of a pure aerosol atmosphere is related to the use of a slightly different molecular profile.

6. Effect of Errors in Reflectance on Aerosol Optical Thickness and Surface Reflectance Retrievals

A. Impact on Aerosol Optical Thickness Retrievals

Several years ago Levy *et al.* [34] conducted a study on the influence of error of scalar simulations on AOT (τ_{aer}) retrievals. The authors calculated LUTs (TOA reflectance values for a number of different atmospheric and geometric conditions) for the MODIS coarse-resolution aerosol retrieval algorithm using the RT3 code in scalar and vector modes. The produced LUTs were then used to derive AOT in the blue and red spectra. Based on the results, they made a conclusion that neglecting the effects of polarization would induce quite large errors (either positive or negative) in individual aerosol retrievals, but would hardly have a significant effect on global and long-term averages. It was also decided to use a vector RT code in future versions of the MODIS aerosol retrieval algorithm.

In this study, we applied a simple analysis to estimate the influence of errors in calculated reflectance values on the accuracy of τ_{aer} retrievals. The term

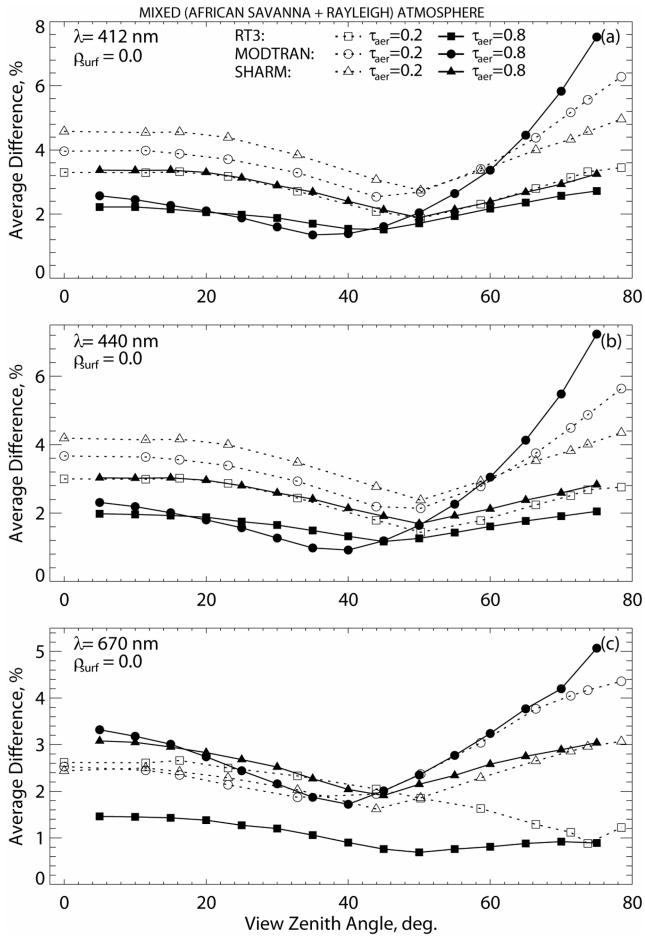

Fig. 9. Results of the comparison of RT3, MODTRAN, and SHARM with 6SV1 for a mixed atmosphere bounded by a black surface. The aerosol constituent is represented by the AS model; $\tau_{mol} = \{0.303; 0.232; 0.042\}$ for $\lambda = \{412; 440; 670\}$nm, respectively. 6SV1 is used as a reference for all codes.

"error" implies all the errors originating from error sources associated with a particular code. For example, in the case of SHARM it is the absence of polarization, while in the case of MODTRAN it is the absence of polarization, the use of the Henyey–Greenstein phase function, and the impossibility of entering an exponential aerosol profile.

Let us assume that we compare benchmark results with the results of a given code as a function of τ_{aer}which are all related to one another through

$$\rho^{bm}(\tau_{aer}) = \rho^{code}(\tau_{aer}) + \Delta\rho^{code}(\tau_{aer}), \qquad (4)$$

where ρ^{bm} is the benchmark TOA reflectance and ρ^{code} and $\Delta\rho^{code}$ are the result and the error of the code under consideration. Since the TOA reflectance is a continuous function of τ_{aer}, we can always find τ^1_{aer} such that

$$\rho^{bm}(\tau_{aer}) = \rho^{code}(\tau^1_{aer}). \qquad (5)$$

On the other hand, it is reasonable to assume that at small variations of τ_{aer} the TOA reflectance is a lin-

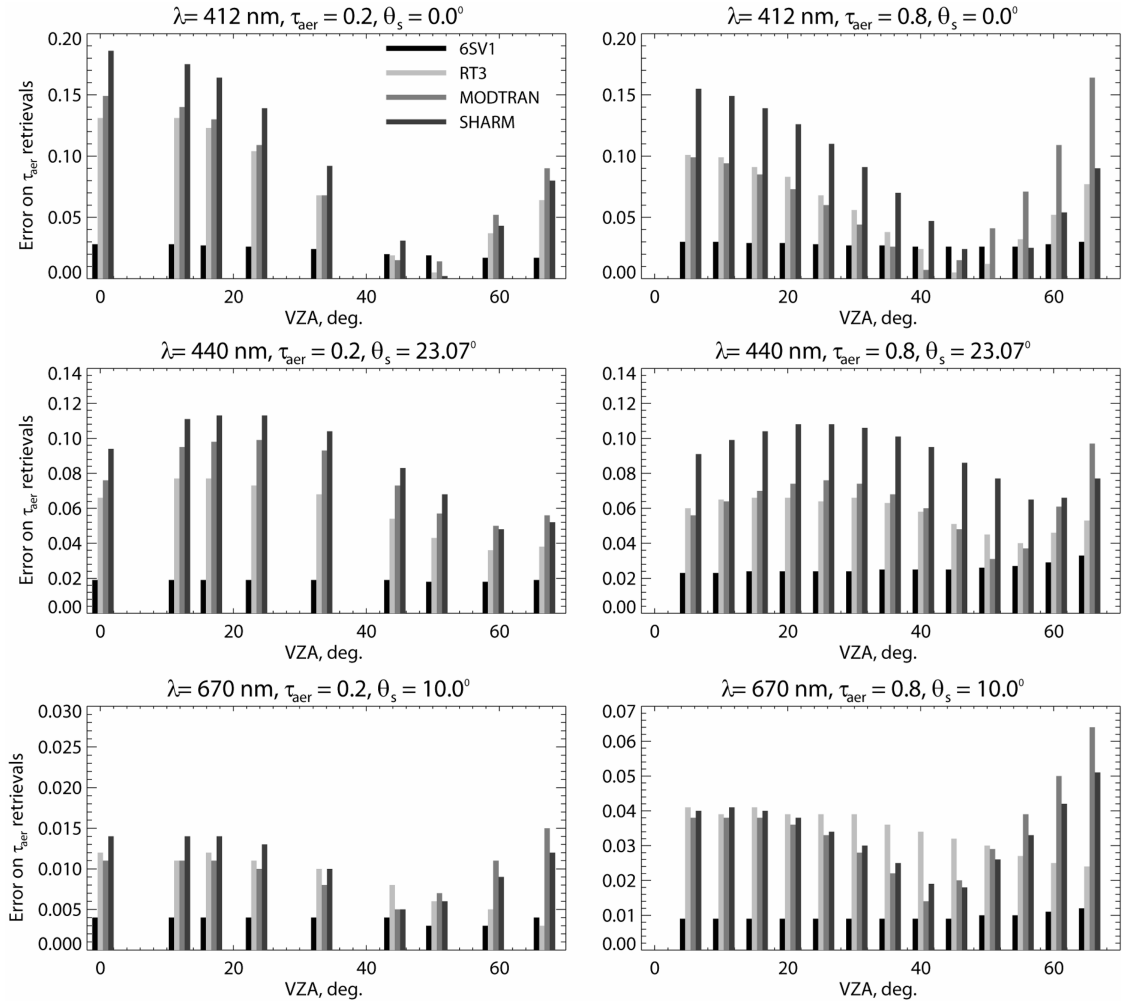

Fig. 10. Errors in AOT (τ_{aer}) retrievals obtained for six cases of a mixed atmosphere bounded by black surface. The aerosol is represented by the AF model. Each error value is averaged over three azimuths, AZ = $\{0.0°; 90.0°; 180.0°\}$.

ear function of τ_{aer}, and $\Delta\rho^{\mathrm{code}}$ can be calculated as

$$\Delta\rho^{\mathrm{code}}(\tau_{\mathrm{aer}}) = \frac{\rho^{\mathrm{code}}(\tau^1_{\mathrm{aer}}) - \rho^{\mathrm{code}}(\tau_{\mathrm{aer}})}{\tau^1_{\mathrm{aer}} - \tau_{\mathrm{aer}}}(\tau^1_{\mathrm{aer}} - \tau_{\mathrm{aer}}) \equiv \alpha(\tau_{\mathrm{aer}})\Delta\tau_{\mathrm{aer}}, \quad (6)$$

where $\alpha(\tau_{\mathrm{aer}})$ is the derivative of $\rho^{\mathrm{code}}(\tau_{\mathrm{aer}})$ and $\Delta\tau_{\mathrm{aer}}$ is the error of τ_{aer} retrieval, which needs to be estimated. Thus, Eq. (4) can be rewritten as

$$\rho^{\mathrm{bm}}(\tau_{\mathrm{aer}}) = \rho^{\mathrm{code}}(\tau_{\mathrm{aer}}) + \alpha(\tau_{\mathrm{aer}})\Delta\tau_{\mathrm{aer}}, \quad (7)$$

and the AOT retrieval error can be estimated from Eq. (7) as

$$\Delta\tau_{\mathrm{aer}} = \frac{\rho^{\mathrm{bm}}(\tau_{\mathrm{aer}}) - \rho^{\mathrm{code}}(\tau_{\mathrm{aer}})}{\alpha(\tau_{\mathrm{aer}})}. \quad (8)$$

The assumption of linearity used here was briefly tested by using SHARM. We simulated TOA reflectance for four slightly different values of $\tau_{\mathrm{aer}} = \{0.2; 0.22; 0.25; 0.27\}$, $\lambda = 412$ nm, and AS aerosol constituent and built it as a function of τ_{aer} for four different values of VZA = $\{0.0°; 16.26°; 32.86°; 50.21°\}$. The corresponding picture is provided on the project Web site [19]. For all VZA, the TOA reflectance varies as a linear function of τ_{aer}.

To calculate the derivative $\alpha(\tau_{\mathrm{aer}})$, we assumed a small variation of 0.05 for each value of τ_{aer} used in this study. Thus, for all cases of a mixed atmosphere bounded by black surface we performed additional calculations with $\tau_{\mathrm{aer}} = \{0.25; 0.85; 2.05\}$ (where applicable).

6SV1 served as a benchmark for RT3, MODTRAN, and SHARM. The accuracy of retrievals made by 6SV1 itself was estimated based on the results of its comparison with Monte Carlo. According to these results, the overall accuracy of 6SV1 is 1%. Thus, to produce "erroneous" 6SV1 results, we added a random 1% noise to the 6SV1 simulations.

Some of the obtained results are shown in Fig. 10. We selected six different cases of a mixed atmosphere with the AF aerosol constituent: $\lambda = 412$ nm, SZA = 0.0°, $\tau_{\mathrm{aer}} = 0.2$ and $\tau_{\mathrm{aer}} = 0.8$; $\lambda = 440$ nm, SZA = 23.0°, $\tau_{\mathrm{aer}} = 0.2$ and $\tau_{\mathrm{aer}} = 0.8$; and $\lambda = 670$ nm, SZA = 10.0°, $\tau_{\mathrm{aer}} = 0.2$ and $\tau_{\mathrm{aer}} = 0.8$. Each plot shows the

azimuth-averaged AOT retrieval error calculated as an average for AZ $= \{0.0°; 90.0°; 180.0°\}$ as a function of VZA. The results for all other cases are stored on the project Web site [19] in the form of Excel files.

The 6SV1 AOT retrieval error is almost negligible for all considered cases. It does not exceed 0.025 for the plots for $\tau_{aer} = 0.2$ and 0.04 for the plots for $\tau_{aer} = 0.8$, which proves the suitability of the code for AOT retrieval operations. The situation is worse for the other codes, which demonstrate relatively large AOT retrieval errors at $\lambda = 412$ nm and $\lambda = 440$ nm. These errors specify the variation range of AOT and thus are critical for small AOT values. For example, according to the results of the second plot on the left (Fig. 10), the error of the retrieved τ_{aer} of 0.2 is 0.11. In general, MODTRAN demonstrates slightly better behavior than SHARM except for large VZA angles, and RT3 shows better behavior than MODTRAN.

Since the largest error arises from ignoring the effects of polarization, the main question is, is it important to use a vector code for AOT (and other aerosol properties) retrievals? It is undoubtedly important from a theoretical point of view, but further analysis is required to estimate its influence on retrieval algorithms. The point is that such algorithms are based on a number of assumptions, and the error arising from the use of these assumptions may exceed the error related to the use of a scalar code. For example, the MAIAC algorithm, which relies on SHARM, assumes invariability of the surface for 16 days and uses a preassigned set of three aerosol models. On the other hand, the internal MODIS AOT algorithm, which is based on 6SV1, assumes a precomputed empirical ratio between reflectance in visible and short-wavelength infrared channels and uses a preassigned set of four aerosol models. Thus, the best solution here would be to calculate a final product error budget. However, the user of a vector code has the advantage of skipping the part related to the accuracy of an underlying RT code.

B. Impact on Surface Reflectance Retrievals

The same approach was applied to estimate the impact of code errors on surface reflectance retrievals, assuming accurate knowledge of the atmospheric aerosol component and a Lambertian surface model. We simply replace τ_{aer} in Eq. (8) with the ρ_{surf} parameter, i.e.,

$$\Delta\rho_{surf} = \frac{\rho^{bm}(\rho_{surf}) - \rho^{code}(\rho_{surf})}{\alpha(\rho_{surf})}. \quad (9)$$

Again, 6SV1 served as benchmark for the other RT codes, and the accuracy of 6SV1 itself was believed to be 1% according to the results of its comparison with Monte Carlo code. To produce the derivative $\alpha(\rho_{surf})$, we reprocessed all mixed atmosphere cases for $\rho_{surf} = 0.04$.

Some of the obtained results are presented in Fig. 11. Here we show the same cases as in Fig. 9 but bounded by a Lambertian surface with $\rho_{surf} = 0.05$. Again, 6SV1 demonstrates very good behavior. Its surface reflectance retrieval error does not exceed 0.005 for all the considered cases. RT3, MODTRAN, and SHARM produce satisfactory results (with the error not exceeding 0.005) for $\lambda = 670$ nm and $\tau_{aer} = 0.2$. In the case of SZA $= 0.0°$ (left- and right-hand plots in the first row) the accuracy of their surface reflectance retrievals is sensitive to the geometric configurations. Thus, they show really small errors for $40.0° \le$ VZA $\le 50.0°$. RT3 is characterized by smaller errors than MODTRAN and SHARM for $\lambda = 412$ and $\lambda = 440$ nm.

In contrast to AOT retrievals, it is important to use a vector code for ρ_{surf} retrievals from both theoretical and experimental points of view. The accuracy of LUTs and, therefore, the accuracy of retrievals themselves directly depend on RT code simulations.

7. Conclusions

We have briefly described the results of a large project devoted to the comparison of four RT codes, including 6SV1, RT3, MODTRAN, and SHARM, used for different remote sensing applications. We evaluated the accuracy of the codes for several realistic atmospheric scenarios by comparing their simulations with those produced by two well-known benchmarks, namely, Coulson's tabulated values [18] and Bréon's Monte Carlo code [4]. We also estimated the influence of the accuracy of each code on AOT and surface reflectance retrieval with the help of a simple theoretical approach. Here we did not consider other characteristics of a RT code, such as speed or user friendliness. Brief information regarding these characteristics can be found on the Web site [19].

6SV1 demonstrated the best agreement with Monte Carlo. The results of this study are consistent with the findings of the previous code validation studies, where the accuracy of a β version of the vector 6S was stated to be within 1%. Since it is not very convenient to use Monte Carlo in code validation and comparison studies because of the angular discretization and large amounts of calculation time, it was decided to create a reference data set, which can be used in further studies, on the basis of 6SV1. The created data set is available on the project Web site [19] and includes all cases considered in this study.

The main source of error in code SHARM is the absence of polarization, which sometimes reduces its accuracy to 7%. MODTRAN demonstrates a slightly better agreement than SHARM for the considered cases of a mixed atmosphere. It seems that the three different sources of disagreement, described in Subsection 5.B.2, well compensate each other and bring the accuracy of MODTRAN to the level of SHARM. Hopefully, two of these sources, namely, the neglect of polarization and inaccurate aerosol modeling, will be successfully eliminated from the next versions of the code, considering the fact that the polarized version of MODTRAN is currently under development and that there is a subsequent version of MODTRAN

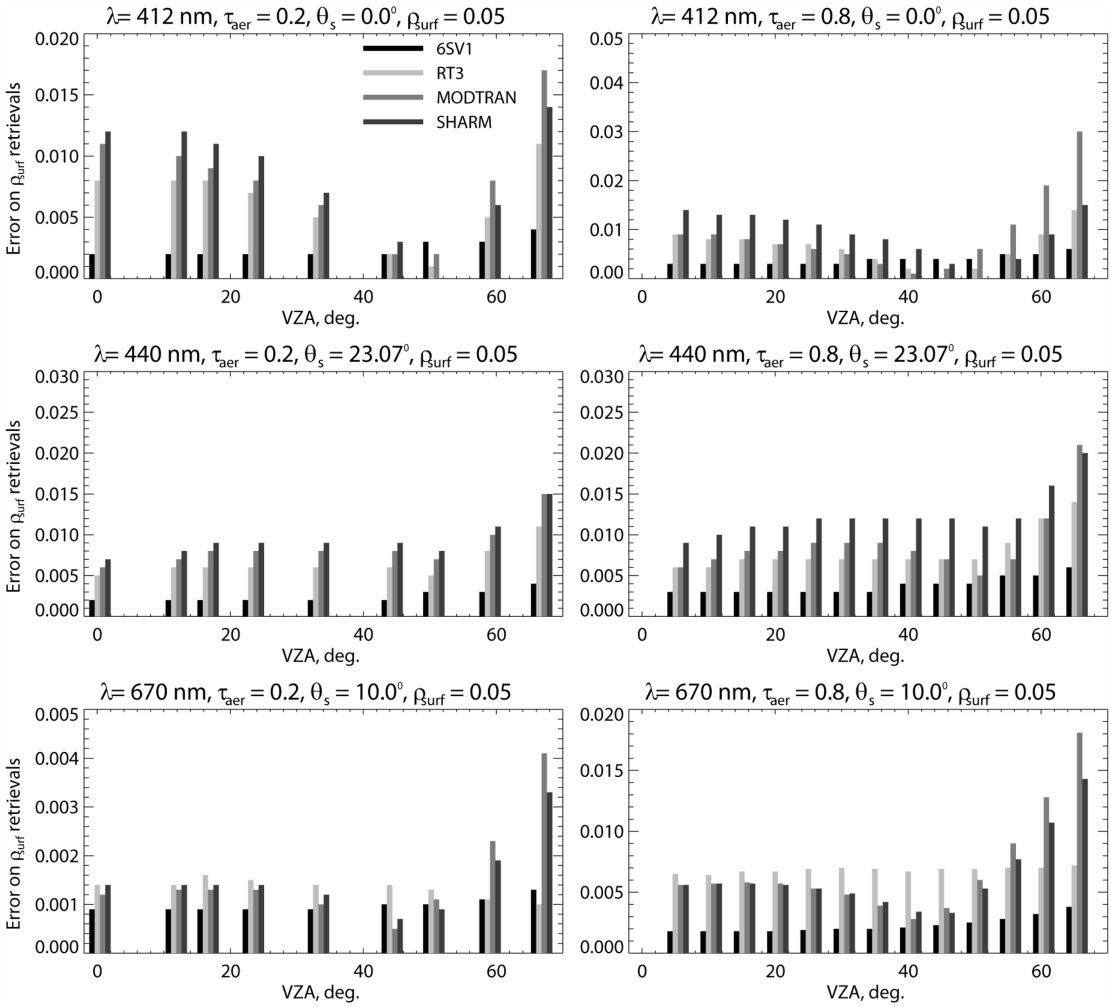

Fig. 11. Errors in surface reflectance (ρ_{surf}) retrievals obtained for six cases of a mixed atmosphere bounded by a Lambertian surface with the reflectance of 0.05. The aerosol is presented by the AF model. Each error value is averaged over three azimuths, AZ = {0.0°; 90.0°; 180.0°}.

(MODTRAN 5 version 3, not publicly available yet) that tackles the aerosol modeling problem by offering the user the opportunity to enter 64 Legendre coefficients. Thus, this code should be reevaluated again in the future.

The disagreement between RT3 and 6SV1 is attributed mainly to the impossibility of inputting user-defined values of VZA and to a relatively small maximum number of calculation angles used in the comparison. A larger number of angles may let one achieve a higher level of accuracy.

In general, the evaluation of the accuracy of a RT code is the first step in creating an atmospheric correction or aerosol retrieval algorithm. However, users of an accurate RT code have the advantage of skipping this part and moving directly to the evaluation of other sources of errors in the resulting product. In addition, the accuracy of an underlying RT code is important for LUTs that include direct RT simulations.

We also mention that all RT codes involved in this study used aerosol phase functions that were calculated on the basis of the Mie theory for homogeneous spheres. Such an assumption of sphericity is not valid for desert dust aerosols, which consist of mainly nonspherical particles with aspect ratios ~1.5. In addition, polarization does have some sensitivity to nonsphericity, especially in the case of coarse mode aerosols [35].

References

1. E. F. Vermote, N. Z. El Saleous, and C. O. Justice, "Atmospheric correction of MODIS data in the visible to middle infrared: first results," Remote Sens. Environ. **83**, 97–111 (2002).
2. A. Lyapustin and Y. Wang, "MAIAC: multi-angle implementation of atmospheric correction for MODIS," Algorithm Theoretical Basis Document, http://neptune. gsfc.nasa.gov/bsb/subpages/index.php?section=Projects&content=MAIAC%20ATDB (2007), p. 69.
3. P. Y. Deschamps, M. Herman, and D. Tanré, "Modeling of the atmospheric effects and its application to the remote sensing of ocean color," Appl. Opt. **22**, 3751–3758 (1983).
4. F.-M. Bréon, "Reflectance of broken cloud fields: simulation and parameterization," J. Atmos. Sci. **49**, 1221–1232 (1992).
5. J. Lenoble, ed., *Radiative Transfer in Scattering and absorbing Atmospheres: Standard Computational Procedures* (A. Deepak, 1985).

6. A. Lyapustin, "Radiative transfer code SHARM-3D for radiance simulations over a non-Lambertian nonhomogeneous surface: intercomparison study," Appl. Opt. **41**, 5607–5615 (2002).
7. M.-J. Kim, G. M. Skofronick-Jackson, and J. A. Weiman, "Intercomparison of millimeter-wave radiative transfer models," IEEE Trans. Geosci. Remote Sens. **42** (9), 1882–1890 (2004).
8. R. F. Cahalan, L. Oreopoulos, A. Marshak, K. F. Evans, A. Davis, R. Pincus, K. Yetzer, B. Mayer, R. Davies, T. Ackerman, H. Barker, E. Clothiaux, R. Ellingson, M. Garay, E. Kassianov, S. Kinne, A. Macke, W. O'Hirok, P. Partain, S. Prigarin, A. Rublev, G. Stephens, F. Szczap, E. Takara, T. Várnai, G. Wen, and T. Zhuravleva, "The I3RC: bringing together the most advanced radiative transfer tools for cloudy atmospheres," Bull. Am. Meteorol. Soc. **86**, 1275–1293 (2005)..
9. J.-L. Widlowski, M. Taberner, B. Pinty, V. Bruniquel-Pinel, M. Disney, R. Fernandes, J.-P. Gastellu-Etchegorry, N. Gobron, A. Kuusk, T. Lavergne, S. Leblanc, P. E. Lewis, E. Martin, M. Mõttus, P. R. J. North, W. Qin, M. Robustelli, N. Rochdi, R. Ruiloba, C. Soler, R. Thompson, W. Verhoef, M. M. Verstraete, and D. Xie, "Third radiation transfer model intercomparison (RAMI) exercise: documenting progress in canopy reflectance models," J. Geophys. Res. **112**, D09111 (2007) .
10. T. Z. Muldashev, A. I. Lyapustin, and U. M. Sultangazin, "Spherical harmonics method in the problem of radiative transfer in the atmosphere–surface system," J. Quant. Spectrosc. Radiat. Transfer **61**, 393–404 (1999).
11. S. Y. Kotchenova and E. F. Vermote, "A vector version of the 6S radiative transfer code for atmospheric correction of satellite data: an Overview," presented at 29th Review of Atmospheric Transmission Models Meeting, Lexington, Mass., USA, (13–14 June 2007).
12. K. F. Evans and G. L. Stephens, "A new polarized atmospheric radiative transfer model," J. Quant. Spectrosc. Radiat. Transfer **46**, 413–423 (1991).
13. R. C. Levy, L. A. Remer, S. Mattoo, E. F. Vermote, and Y. Kaufman, "Second-generation algorithm for retrieving aerosol properties over land from MODIS spectral reflectance," J. Geophys. Res. **112**, D13211 (2007). .
14. A. Berk, G. P. Anderson, L. S. Bernstein, P. K. Acharya, H. Dothe, M. W. Matthew, S. M. Adler-Golden, J. H. Chetwynd, Jr., S. C. Richtsmeier, B. Pukall, C. L. Allred, L. S. Jeong, and M. L. Hoke, "MODTRAN4 radiative transfer modeling for atmospheric correction," Proc. SPIE **3756**, 348–353 (1999).
15. P. K. Acharya, A. Berk, G. P. Anderson, N. F. Larsen, S.-C. Tsay, and K. H. Stamnes, "MODTRAN 4: multiple scattering and bi-directional reflectance distribution function (BRDF) upgrades to MODTRAN," Proc. SPIE **3756**, 354–362 (1999).
16. A. Berk, L. S. Bernstein, G. P. Anderson, P. K. Acharya, D. C. Robertson, J. H. Chetwynd, and S. M. Adler-Golden, "MODTRAN cloud and multiple scattering upgrades with application to AVIRIS," Remote Sens. Environ. **65**, 367–375 (1998).
17. A. I. Lyapustin, "Radiative transfer code SHARM for atmospheric and terrestrial application," Appl. Opt. **44**, 7764–7772 (2005).
18. K. L. Coulson, J. V. Dave, and Z. Sekera, *Tables Related to Radiation Emerging from a Planetary Atmosphere with Rayleigh Scattering* (U. California Press, 1960).
19. "Official code comparison Web site of the MODIS atmospheric correction group," http://rtcodes.ltdri.org.
20. S. Y. Kotchenova, E. F. Vermote, R. Matarrese, and F. Klemm, "Validation of a vector version of the 6S radiative transfer code for atmospheric correction of satellite data. Part I: path radiance," Appl. Opt. **45**, 6762–6774 (2006).
21. S. Y. Kotchenova and Vermote, "Validation of a vector version of the 6S radiative transfer code for atmospheric correction of satellite data. Part II: Lambertian and anisotropic surfaces," Appl. Opt. **46**, 4455–4464 (2007).
22. E. F. Vermote, D. Tanré, J. L. Deuzé, M. Herman, J. J. Morcrette, S. Y. Kotchenova, and T. Miura, Second simulation of the satellite signal in the solar spectrum (6S), 6S user guide version 3, November 2006, http://6s.ltdri.org.
23. K. Stamnes, S.-C. Tsay, W. Wiscombe, and K. Jayaweera, "Numerically stable algorithm for discrete-ordinate method radiative transfer in multiple scattering and emitting layered media," Appl. Opt. **27**, 2502–2509 (1988).
24. K. Stamnes, S.-C. Tsay, W. Wiscombe, and I. Laszlo, "DISORT, a general-purpose FORTRAN program for discrete-ordinate-method radiative transfer in scattering and emitting layered media: documentation of methodology," version 1.1 (March 2000), available as "DISORTReport1.1.pdf" at ftp://climate1.gsfc.nasa.gov/wiscombe/Multiple_Scatt/.
25. E. Vermote and D. Tanré, "Analytical expressions for radiative properties of planar Rayleigh scattering media, including polarization contributions," J. Quant. Spectrosc. Radiat. Transfer **47**, 305–314 (1992).
26. B. M. Herman, T. R. Caudill, D. E. Flittner, K. J. Thome, and A. Ben-David, "Comparison of the Gauss–Seidel spherical polarized radiative transfer code with other radiative transfer codes," Appl. Opt. **34**, 4563–4572 (1995).
27. K. Masuda, "Infrared sea surface emissivity including multiple reflection effect for isotropic Gaussian slope distribution model," Remote Sens. Environ. **103**, 488–496 (2006).
28. M. I. Mishchenko, A. A. Lacis, and L. D. Travis, "Errors induced by the neglect of polarization in radiance calculations for Rayleigh-scattering atmospheres," J. Quant. Spectrosc. Radiat. Transfer **51**, 491–510 (1994).
29. A. A. Lacis, J. Chowdhary, M. I. Mishchenko, and B. Cairns, "Modeling errors in diffuse-sky radiation: vector vs. scalar treatment," J. Geophys. Res. **25**,135–138 (1998).
30. O. Dubovik, B. Holben, T. F. Eck, A. Smirnov, Y. J. Kaufman, M. D. King, D. Tanré, and I. Slutsker, "Variability of absorption and optical properties of key aerosol types observed in worldwide locations," J. Atmos. Sci. **59**, 590–608 (2002).
31. N. C. Hsu, S.-C. Tsay, M. D. King, and J. R. Herman, "Aerosol properties over bright-reflecting source regions," IEEE Trans. Geosci. Remote Sens. **42**, 557– 569 (2004).
32. W. Wiscombe, "Improved Mie scattering algorithms," Appl. Opt. **19**, 1505–1509 (1980).
33. E. Shettle, Remote Sensing Division Code 7227, Naval Research Laboratory, Washington, DC 20375-5351 (personal communication, 2 October 2007).
34. R. C. Levy, L. A. Remer, and Y. J. Kaufman, "Effects of neglecting polarization on the MODIS aerosol retrieval over land," IEEE Trans. Geosci. Remote Sens. **42**, 2576–2583 (2004).
35. O. Dubovik, A. Sinyuk, T. Lapyonok, B. N. Holben, M. Mishchenko, P. Yang, T. F. Eck, H. Volten, O. Muňoz, B. Veihelmann, W. J. van der Zande, J.-F. Leon, M. Sorokin, and I. Slutsker, "Application of spheroid models to account for aerosol particle non-sphericity in remote sensing of desert dust," J. Geophys. Res. **111**, 1–34 (2006).